Songklanakarin J. Sci. Technol.
35 (4), 469-482, Jul. - Aug. 2013

SJST SONGKLANAKARIN JOURNAL OF SCIENCE AND TECHNOLOGY
http://www.sjst.psu.ac.th

Review Article

Petrochemistry and origin of basalt breccia from Ban Sap Sawat area, Wichian Buri, Phetchabun, central Thailand

Phisit Limtrakun[1,*], Yuenyong Panjasawatwong[1], and Jongkonnee Khanmanee[2]

[1] *Department of Geological Sciences, Faculty of Science, Chiang Mai University, Mueang, Chiang Mai, 50200 Thailand.*

[2] *Department of Mineral Resources, Rama 6 Road, Bangkok, 10400 Thailand.*

Received 9 October 2012; Accepted 13 May 2013

Abstract

Thailand is usually considered to be controlled by escape tectonics associated with India-Asia collision during the Late Cenozoic, and basaltic volcanism took place in this extensional period. This volcanism generated both subaqueous and subaerial lava flows with tholeiitic to alkalic basaltic magma. The subaqueous eruptions represented by the studied Wichian Buri basalts, Ban Sap Sawat in particular, are constituted by two main types of volcanic lithofacies, including lava flows and basalt breccias. The lava flows are commonly porphyritic with olivine and plagioclase phenocrysts and microphenocrysts, and are uncommonly seriate textured. The basalt breccias are strongly vitrophyric texture with olivine and plagioclase phenocrysts and microphenocrysts. Chemical analyses indicate that both lava flows and basalt breccias have similar geochemical compositions, signifying that they were solidified from the same magma. Their chondrite normalized REE patterns and N-MORB normalized patterns are closely analogous to the Early to Middle Miocene tholeiites from central Sinkhote-Alin and Sakhalin, northeastern margin of the Eurasian continent which were erupted in a continental rift environment. The origin for the Wichian Buri basalts show similarity of lava flows and basalt breccias, in terms of petrography and chemical compositions, signifying that they have been formed from the same continental within-plate, transitional tholeiitic magma.

Keywords: cenozoic, petrology, geochemistry, intraplate, basalt breccia

1. Introduction

The Late Cenozoic basalts in mainland Southeast Asia range in age from 24 Ma to less than 1 Ma and form a large continental volcanic province. In Thailand and western Cambodia, exposures of the Late Cenozoic basalts are generally small and scattered, whereas those in eastern Cambodia and southern Laos as well as central and southern Vietnam tend to be larger and more extensive. The Late Cenozoic basalts also occur in other parts of Asia including southeastern China, central Burma and Malaysia Peninsula. The Southeast Asian basalts have diverse geochemistry ranging from tholeiitic to strongly alkalic affinities, including mugearites, hawaiites, alkali olivine basalts, basanites and nephelinites (Barr and MacDonald, 1981; Tu *et al.*, 1991; Tu *et al.*, 1992; Flower *et al.*, 1992; Hoang *et al.*, 1996; Hoang and Flower, 1998; Ho *et al.*, 2000; Sutherland *et al.*, 2002; Graham *et al.*, 2008; Wang *et al.*, 2012).

In Thailand, each basalt occurrence is named after the local district or city where it occurs. They are exposed in northern, central, western, eastern and southeastern parts of Thailand (Figure 1). Several localities of these basalts are regarded as the sources of gem-quality corundum, which are usually found in alluvial deposits adjacent to basalt outcrops. Gem-quality corundum is most commonly associated with strongly alkalic basalt that contains abundant peridotitic mantle xenoliths. Many geochemical studies have been published on basalts from Thailand over the last two decades.

* Corresponding author.
Email address: phisit.l@cmu.ac.th

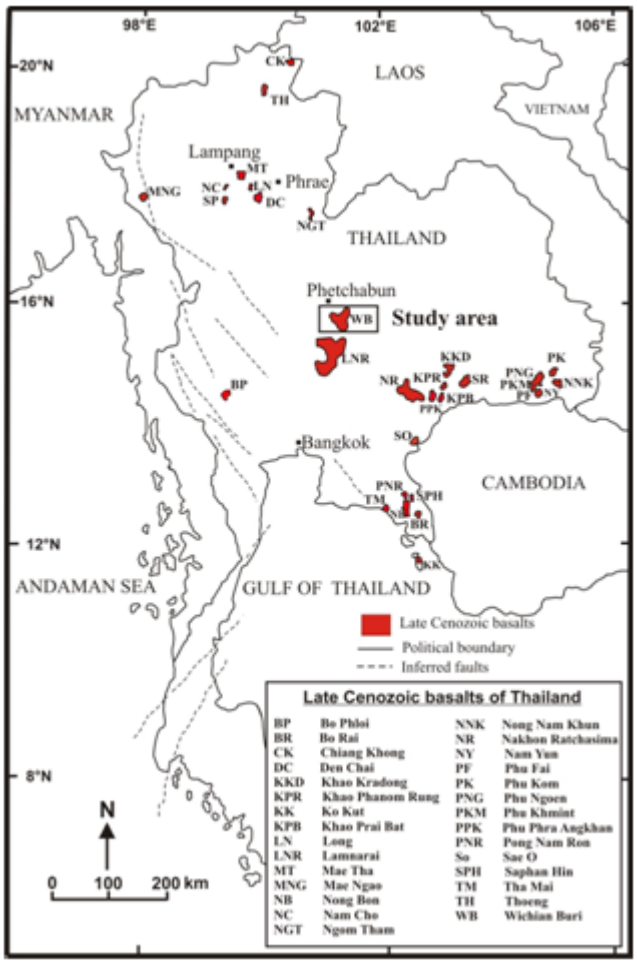

Figure 1. Distributions of Late Cenozoic basalts in Thailand and the study area (Limtrakun *et al.*, 2005).

They are predominantly alkalic to tholeiitic in character and their ages range from 8 Ma to less than 0.5 Ma (Sutthirat *et al.*, 1994; Intasopa *et al.*, 1995).

Late Cenozoic volcanism in Southeast Asia began at least 8 Ma and has continued to the present time. No systematic relationship appears to exist between age and geographic location, and volcanic activity seems to be randomly distributed throughout the region. Southeast Asia is also a region of complex tectonics (Tingay *et al.*, 2010). Several synchronous events may have influenced the tectonics of the area in late Cenozoic, including opening of the South China Sea (Ben-Avraham and Uyeda, 1973), opening of the Andaman Sea (Lawver *et al.*, 1976) and the collision between the Indian and Eurasia plates (Tapponnier et al., 1986). The Late Cenozoic basalts in mainland Southeast Asia may, therefore, be a surface expression of these complex regional tectonic events in this region, mostly driven by escape tectonics related to the collision of India and Asia (Yin, 2010; Xia *et al.*, 2011). Escape tectonics was a major influence in the areas of Southeast Asia in late Oligocene to Recent (Morley *et al.*, 2001; Morley, 2002). The dominant deformation during this period was strike slip faulting. These structures were grossly compressional initially, but crustal extension started in Thailand during the Miocene (Dunning *et al.*, 1995), and most of the basalts date from this extensional period.

The study area is located in the Loei-Phetchabun volcanic belt, covering an area of approximately 300 km^2 in the Wichian Buri District, Phetchabun Province, Central Thailand (Figure 1). The first goal of this study is to characterize basaltic lava flows and basalt breccias from both outcrops and drill holes in terms of lithology, petrography and whole rock geochemistry, and to perform logging and facies analysis of available core samples. The second goal is to outline an episode of this volcanism by combining the result of this study with previous data to correlate relationships between it and the neotectonic evolution in the region. These data are integrated to give a new view to the origin of the basalt breccias in the area.

2. Geologic Setting

The study area is constituted by a number of rock units from Permian to recent (Figure 2) as described in the geologic map of Jungyusuk and Sinsakul (1989). The Permian rocks can be divided into three formations from bottom to top as follows: the Khao Luak formation, the Tak Fa formation and the Hua Na Kham formation. They have ages in the range of Lower to Middle Permian. The lower unit includes abundant black shale and slaty shale and minor yellowish brown sandstone and gray crystalline limestone lenses. The middle unit is made up of thinly bedded or massive limestone with bedded chert and shale. This unit contains abundant fusulinids, corals, brachiopods and bryozoans of the Lower to Middle Permian. The upper unit comprises sandstone, siltstone, shale, limestone, tuff and agglomerate. This rock unit was locally intruded by andesitic plutonic rocks.

The Mesozoic rocks cover a narrow area in the western part and are known as the Huai Sai formation. They consist of reddish brown sandstone that shows cross lamination and basal conglomerate that contains clasts of quartz, chert, sandstone, limestone and volcanic rocks. The Tertiary sediments are known as the Nam Duat formation. They are made up of semiconsolidated sandstone interbedded with shale. The Quaternary sediments comprise alluvial and terrace deposits.

Igneous rocks in the area are divided into two groups: with ages of (1) Permian to Triassic and (2) Tertiary. The older age rocks are phyric basalt and andesite with shallow intrusive diorite. The younger rocks include trachyte porphyry and basalt. The basalts contain ultramafic xenoliths and megacrysts of spinel. Pillow lobes and pillow fragments with radial joints and glassy skins are also observed.

3. Sample Collection

Field work was conducted in 2007 when the basaltic rocks were collected from lava flows or dense clasts in basalt

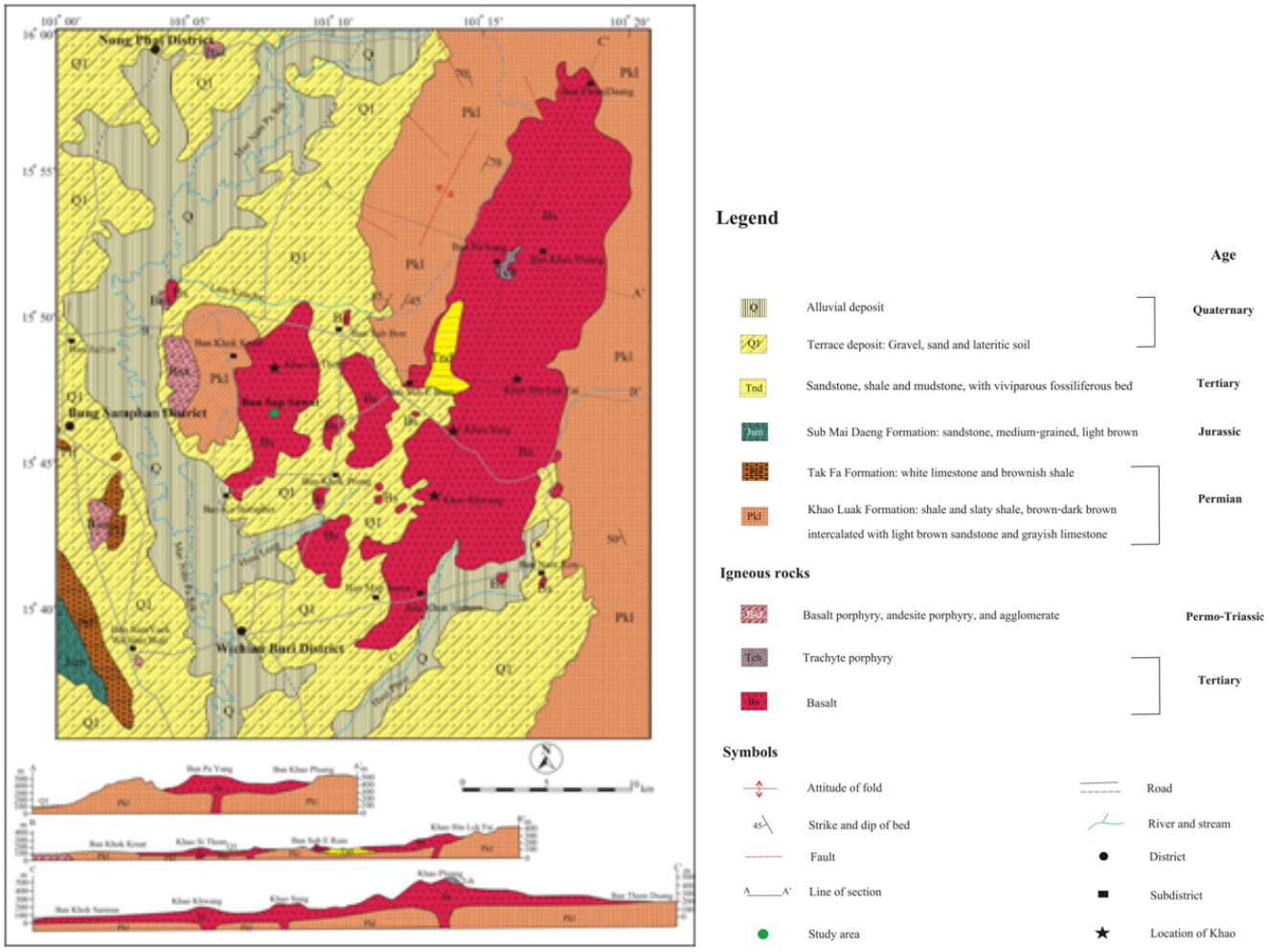

Figure 2. Regional geological map showing distribution of the Late Cenozoic Wichian Buri basalts (Jungyusuk and Sinsakul, 1989).

breccias including 13 outcrop samples of coherent facies basaltic lava flows and 33 core samples from 5 drill holes which were drilled by the Department of Mineral Resources of Thailand in 2005. Of the core samples, 3 samples are coherent facies basaltic lava flows, 19 samples are coherent facies basaltic clasts (>64 mm across) in the basalt breccias, and 11 samples are incoherent facies basaltic clasts (5-64 mm across) in the basalt breccias (Figures 3 and 4). In this study, coherent facies and incoherent facies were namely followed the nomenclature given by McPhie *et al.* (1993). The coherent facies rocks comprise dark gray to grayish black lava flows. The incoherent facies rocks are of basalt breccias that shows either jigsaw fit textures or poorly sorted fabric, angular to round mafic volcanic fragments, and fine grained with glassy matrix. These selected samples are considered to be least-altered under the petrographic microscope, characterized by the scarcity of (1) extensive development of mesoscopic domains of secondary minerals, for example quartz resulted from silicification, epidote minerals and chlorite, (2) abundant vesicles or amygdule minerals, xenocrysts and xenoliths, and (3) quartz, epidote or calcite veining or patches totaling more than 5 modal %. Using the above criteria, 46 least-altered samples were carefully selected to examine their whole-rock geochemistry.

4. Petrography

4.1 Outcrop samples

Most samples have textures varying from slightly to moderately porphyritic with a sample displaying seriate texture (WB13). The common phenocryst (>0.3 mm across) assemblage is plagioclase and olivine. They form isolated crystals, glomerocrysts and cumulocrysts in a fine grained holocrystalline groundmass which shows a felty texture. The groundmass comprises plagioclase, olivine, clinopyroxene and minor titanomagnetite. Ophitic to subophitic intergrowths between plagioclase and clinopyroxene have been also observed in the groundmass. Plagioclase is subhedral and displays twinning and zonation. Determination of plagioclase anorthite content (An–content) on the basis of petrographic techniques shows that they range from oligoclase to

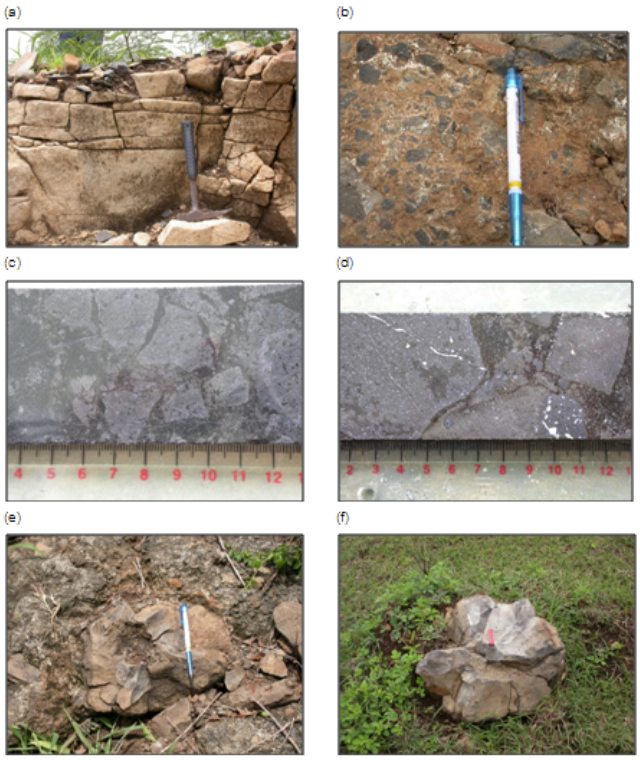

Figure 3. Photographs of the basaltic lava flows (a), the basalt breccias (b), core samples of basalt breccias that show jigsaw-fit texture (c and d), pillow fragments (e and f).

bytownite. Olivine with spinel inclusions are anhedral to subhedral displaying disequilibrium features and have been variably altered to chlorite and serpentine.

4.2 Core samples

Similar features to the outcrop samples were also observed in the clasts of basalt breccias. They exhibit porphyritic and vitrophyric textures with only one seriate texture (WB14). These rocks contain phenocrysts and microphenocrysts of plagioclase and olivine. The groundmass textures range from holocrystalline, felty to hypohyaline and glassy consisting of plagioclase, olivine, clinopyroxene, titanomagnetite, volcanic glass and quench crystals of olivine and plagioclase. The groundmass of volcanic glass has been commonly replaced by dark brown to bluish green palagonite. Plagioclase grains have subhedral outlines and complex zonation. The An–content of plagioclase vary from andesine to bytownite. Olivine crystals with spinel inclusions show a sieve texture and an embayed outline.

5. Geochemistry

5.1 Sample preparation

The 46 selected samples were prepared for whole-rock chemical analyses by splitting into conveniently sized fragments, and then crushing to small chips (~5 mm across), using a hydraulic splitter-crusher (Rocklabs, Auckland, New Zealand). The chips were chosen to avoid vesicles, amygdale minerals, veinlets, xenocrysts, xenoliths and weathering surfaces. The selected chips were blown by compressed air to remove dusty materials. Approximately 50-80 g of the cleaned chips were pulverized for a few minutes by a Rocklabs tungsten carbide ring mill. All the preparation procedures were carried out at the Department of Geological Sciences, Faculty of Science, Chiang Mai University, Thailand.

5.2 Analytical procedures

The whole-rock chemical analyses of major oxides and trace elements (Ba, Rb, Sr, Y, Zr, Nb, V, Ni, Cr, Sc) were performed using X-ray fluorescence (XRF) spectroscopy at the Department of Geological Sciences, Chiang Mai University, Thailand. Major oxides were measured from fusion discs prepared with 0.06 g LiBr, 3.0 g $Li_2B_4O_4$ and 0.6 g sample powder. Trace element analysis was performed on pellets made by pressing the mixtures of 5.0 g sample powder with 0.3 g $C_6H_8O_3N_2$ wax and H_3BO_3. The net (background corrected) intensities were measured and the concentrations were calculated against the calibrations derived from five international standard reference materials (AGV-2, BCR-2, BHVO-2, BIR-1 and RGM-1). The inter-elements matrix corrections were calculated by the SuperQ v3.0 program (Philips). The reporting detection limits are 0.01 wt% for major oxides and 6 ppm for Cr and V, 5 ppm for Ni and Sc, 3 ppm for Rb and 2 ppm for Sr, Y, Zr, Nb and Th. The ignition loss (LOI) was gravimetrically determined by heating 1.0 g sample powder at 1,050°C for 12 hours. The whole-rock chemical analyses for the studied basaltic rocks are given in Table 1.

Eight representative basalts were analyzed for rare earth elements (REE) using inductively coupled plasma mass spectrometry (ICP-MS) housed at the School of Earth Sciences, Royal Holloway College, University of London. Estimated precision is 5-10 % and realistic working detection limit is around 1 ppm for most REE with exception of Er (2 ppm) and Pr (10 ppm). The rare earth elements concentrations and the selected chondrite-normalized ratios for the studied basaltic rocks are given in Table 2.

5.3 Chemical characteristics

All samples have narrow compositional ranges (Table 1) and incompatible element ratios. Both coherent facies basaltic lava flows and the clasts in basalt breccias have similar chemical compositions implying that they are essentially co-magmatic. Although some clasts in the basalt breccias have been partially altered, as illustrated by their modally modified constituents and extremely high LOI content (7.26–19.24 wt%), their chemical compositions are not significantly different from the coherent facies basaltic

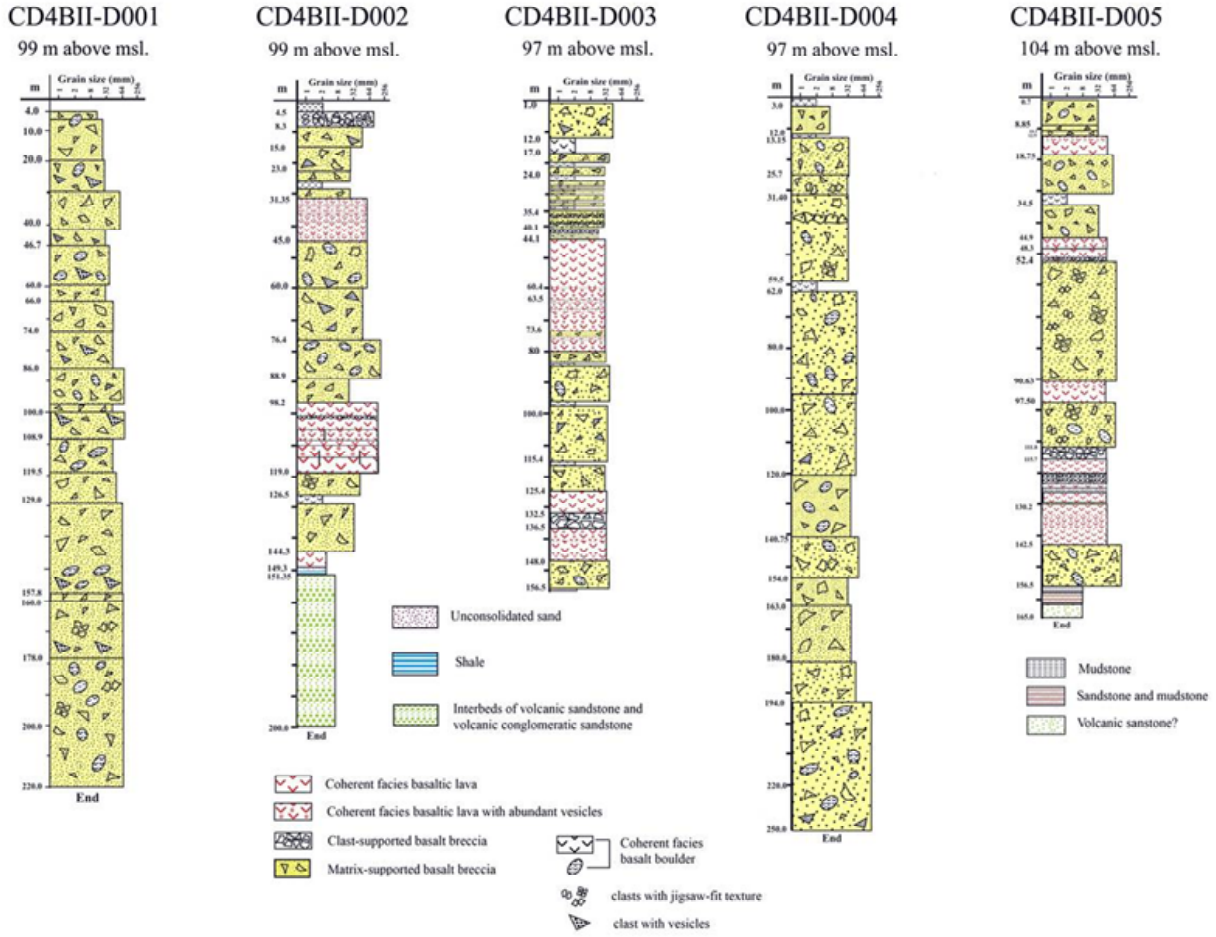

Figure 4. Graphic log of core samples from five drill holes.

samples.

The basalt lavas samples form a compositional field straddling the demarcation line separating an alkalic field from a subalkalic field and are located in the field of basalt on a total alkalis-silica (TAS) diagram (Figure 5). The coherent facies basalts have K_2O/Na_2O ratios varying from 0.09 to 0.26. Those samples with high K_2O/Na_2O ratios (>0.21), are typically those that show greater degrees of alteration (Wang *et al.*, 2010). This is well supported by the higher K_2O/Na_2O values for the incoherent facies basalts (0.14-0.64). The transitional subalkalic-alkalic nature of the studied basalts is consistent with their Nb/Y ratios (0.12-0.38) which are more subalkalic than alkalic (Pearce and Cann, 1973; Floyd and Winchester, 1975; Winchester and Floyd, 1977; Pearce, 1982) (Figure 6). However, their normative nepheline abundances are up to 4.44 wt% (Table 1), characteristic of mildly alkalic rocks. The abundances of SiO_2 and total iron as FeO* and FeO*/MgO ratios (Figure 7) signify that the coherent facies basalts are transitional tholeiite to alkalic basalts rather than transitional calc-alkalic to alkalic basalts.

The proportions of FeO and MgO for the coherent facies basalts correspond to Mg/(Mg+Fe) (mg#) in a range of 0.36-0.45, signifying that they are not representative of

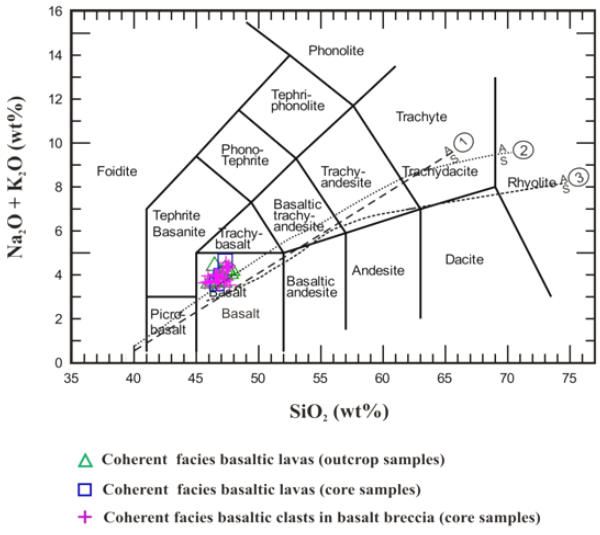

Figure 5. Classification diagram of total alkalis versus silica for the studied basalts; delimited fields for different rock types are taken from Le Bas *et al.* (1986). The field boundaries between alkalic series (A) and subalkalic series (S) of (1) MacDonald (1968), (2) Irvine and Baragar (1971) and (3) Kuno (1966).

Table 1. Whole-rock major and trace element compositions, normalized to 100 wt.% on the basis of volatile free, of the studied basaltic rocks.

Coherent facies basaltic lavas (outcrops)													
Sample	WB1	WB2	WB3	WB4	WB5	WB6	WB7	WB8	WB9	WB10	WB11	WB12	WB13
Major (wt.%)													
SiO_2	47.54	47.75	47.67	48.19	47.87	47.26	46.98	46.58	48.12	47.21	47.18	47.38	47.47
TiO_2	1.56	1.61	1.55	1.53	1.54	1.58	1.53	1.47	1.55	1.38	1.54	1.44	1.43
Al_2O_3	16.57	16.58	16.86	17.10	16.96	17.37	17.43	17.44	16.76	17.27	17.23	17.35	17.21
FeO	10.43	10.33	10.27	9.89	10.11	9.84	10.05	10.10	10.12	10.11	9.91	9.93	10.12
Fe_2O_3	1.88	1.86	1.85	1.78	1.82	1.77	1.81	1.82	1.82	1.82	1.78	1.79	1.82
MnO	0.15	0.16	0.15	0.14	0.14	0.14	0.14	0.14	0.14	0.14	0.14	0.14	0.15
MgO	8.01	7.82	8.07	7.96	7.96	8.26	8.29	8.71	7.86	8.46	8.20	8.18	7.46
CaO	9.34	9.41	9.30	9.06	9.07	9.72	9.74	9.82	9.15	9.63	9.67	9.87	9.39
Na_2O	3.53	3.50	3.34	3.42	3.55	3.14	3.20	3.09	3.53	3.27	3.45	3.18	3.93
K_2O	0.71	0.71	0.66	0.66	0.69	0.63	0.54	0.56	0.67	0.48	0.62	0.47	0.56
P_2O_5	0.28	0.28	0.28	0.28	0.29	0.30	0.30	0.28	0.28	0.24	0.29	0.27	0.45
Total	100.00	100.00	100.00	100.00	100.00	100.00	100.00	100.00	100.00	100.00	100.00	100.00	100.00
LOI	0.64	1.02	1.24	1.64	0.79	1.23	1.45	1.35	1.13	1.10	1.05	1.05	1.71
mg#	0.37	0.37	0.38	0.38	0.38	0.39	0.39	0.40	0.38	0.39	0.39	0.39	0.36
CIPW norms (wt.%)													
Or	4.20	4.20	3.90	3.90	4.08	3.73	3.19	3.31	3.96	2.84	3.67	2.78	3.31
Ab	24.22	24.94	25.47	27.53	26.11	23.80	23.31	21.49	26.84	23.84	22.95	24.47	25.12
An	27.23	27.39	29.02	29.32	28.27	31.40	31.56	32.02	27.87	30.98	29.65	31.64	27.63
Ne	3.04	2.51	1.50	0.75	2.11	1.48	2.02	2.51	1.62	2.06	3.36	1.31	4.39
Di	14.33	14.48	12.69	11.46	12.32	12.32	12.28	12.31	13.02	12.59	13.60	12.89	13.41
Ol	20.68	20.11	21.19	20.95	20.92	21.06	21.45	22.33	20.49	21.91	20.63	21.00	19.8
Mt	2.73	2.70	2.68	2.58	2.64	2.57	2.62	2.64	2.64	2.64	2.58	2.60	2.64
Il	2.96	3.06	2.95	2.91	2.93	3.00	2.91	2.79	2.95	2.62	2.93	2.74	2.72
Ap	0.61	0.61	0.61	0.61	0.63	0.65	0.65	0.61	0.61	0.52	0.63	0.59	0.98
Total	100.00	100.00	100.00	100.00	100.00	100.00	100.00	100.00	100.00	100.00	100.00	100.00	100.00
Trace (ppm)													
Ba	285	274	267	206	290	212	273	264	271	219	206	232	231
Rb	10	11	10	8	12	8	9	8	11	9	8	8	7
Sr	527	508	534	543	537	589	618	592	554	542	567	610	658
Y	33	34	33	21	33	23	35	33	33	35	23	35	24
Zr	141	141	142	141	144	149	151	144	143	138	145	141	157
Nb	8	8	8	8	8	8	8	6	8	4	8	4	7
V	242	251	243	184	237	185	246	232	246	232	182	232	179
Ni	115	121	127	99	117	97	139	145	122	153	100	133	79
Cr	369	336	351	273	330	262	341	350	341	345	241	339	207
Sc	28	35	27	25	30	22	33	26	34	32	20	31	16

LOI = loss on ignition; mg# = molecular MgO/(MgO+FeO); FeO and Fe_2O_3 calculated using Fe_2O_3/FeO = 0.2 from Middlemost (1989)

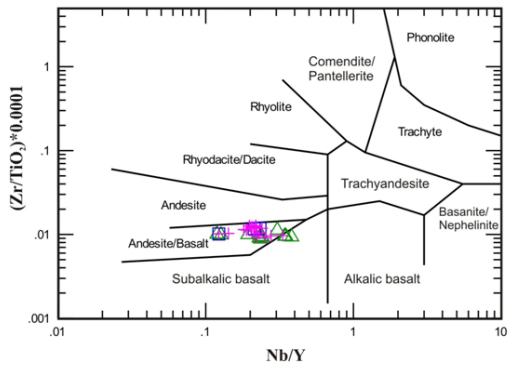

Figure 6. Plot of Zr/TiO_2 versus Nb/Y for the studied basalts and the symbols used as in Figure 5. The field boundaries for different magma types are taken from Winchester and Floyd (1977).

Table 1. Continued

Coherent facies basaltic lavas (cores)				Coherent facies clasts in basalt breccias (cores)							
Sample	WB27	WB30	WB36	WB14	WB17	WB19	WB21	WB22	WB25	WB29	WB32
Major (wt.%)											
SiO_2	47.43	47.92	47.82	46.37	47.53	47.83	48.08	48.37	48.38	48.12	47.42
TiO_2	1.41	1.30	1.30	1.46	1.26	1.27	1.27	1.23	1.27	1.26	1.25
Al_2O_3	17.44	16.98	17.29	17.43	17.42	17.12	17.23	17.23	17.17	17.03	17.29
FeO	9.79	9.72	9.62	9.92	9.57	9.67	9.54	9.48	9.53	9.60	9.78
Fe_2O_3	1.76	1.75	1.73	1.78	1.72	1.74	1.72	1.70	1.71	1.73	1.76
MnO	0.14	0.15	0.15	0.14	0.14	0.15	0.15	0.14	0.14	0.14	0.14
MgO	8.02	8.45	8.52	8.58	8.48	8.61	8.42	8.25	8.42	8.39	8.60
CaO	9.70	8.72	9.59	10.34	9.90	9.53	9.73	8.82	8.43	9.08	9.43
Na_2O	3.49	3.93	3.07	3.33	3.27	3.30	3.06	3.70	3.87	3.53	3.40
K_2O	0.53	0.77	0.60	0.36	0.43	0.49	0.51	0.78	0.78	0.82	0.61
P_2O_5	0.29	0.31	0.31	0.29	0.27	0.28	0.31	0.29	0.31	0.30	0.32
Total	100.00	100.00	100.00	100.00	100.00	100.00	100.00	100.00	100.00	100.00	100.00
LOI	0.81	1.39	2.07	1.66	1.22	1.86	1.06	1.44	2.58	2.26	1.94
mg#	0.39	0.40	0.41	0.40	0.41	0.41	0.41	0.40	0.41	0.40	0.41
CIPW norms (wt.%)											
Or	3.13	4.55	3.55	2.13	2.54	2.90	3.02	4.67	4.61	4.85	3.61
Ab	24.11	25.02	25.54	20.38	24.33	25.66	25.86	26.46	27.22	25.18	23.85
An	30.32	26.38	31.58	31.51	31.55	30.42	31.72	28.03	27.13	28.16	30.07
Ne	2.92	4.44	0.22	4.21	1.80	1.21	0.00	2.61	2.97	2.52	2.65
Di	13.19	12.32	11.59	14.79	13.07	12.44	13.26	11.47	10.52	12.37	12.13
Ol	20.47	21.61	21.86	21.00	21.24	21.82	20.56	21.32	21.98	21.36	22.07
Mt	2.55	2.54	2.51	2.58	2.49	2.52	2.49	2.47	2.48	2.51	2.55
Il	2.68	2.47	2.47	2.77	2.39	2.41	2.41	2.34	2.41	2.39	2.38
Ap	0.63	0.68	0.68	0.63	0.59	0.61	0.68	0.63	0.68	0.65	0.70
Total	100.00	100.00	100.00	100.00	100.00	100.00	100.00	100.00	100.00	100.00	100.00
Trace (ppm)											
Ba	244	295	276	266	283	260	269	296	277	290	288
Rb	9	12	10	6	8	8	8	9	12	10	9
Sr	580	517	491	619	485	475	508	535	464	639	517
Y	35	36	36	36	36	35	37	34	36	37	36
Zr	142	150	149	147	143	142	149	149	146	157	149
Nb	4	8	8	4	6	7	8	8	9	7	8
V	235	212	228	251	223	228	226	219	226	212	225
Ni	134	172	163	140	158	167	165	168	176	168	173
Cr	313	365	359	331	361	366	364	350	356	356	364
Sc	32	33	31	34	33	32	31	31	26	35	35

LOI = loss on ignition; mg# = molecular MgO/(MgO+FeO); FeO and Fe_2O_3 calculated using Fe_2O_3/FeO = 0.2 from Middlemost (1989)

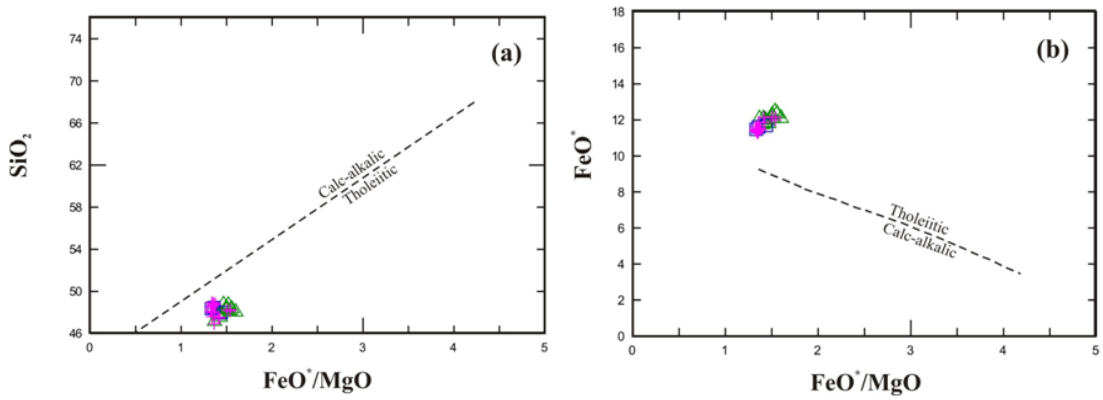

Figure 7. Plots of (a) SiO_2 and (b) FeO^* versus FeO^*/MgO for the studied basalts and the symbols used as in Figure 5. The field boundaries between tholeiitic and calc-alkalic are taken from Miyashiro (1975).

Table 1. Continued

Coherent facies clasts in basalt breccias (cores)											
Sample	WB34	W35	WB38	WB40	WB41	WB42	WB43	WB44	WB46	WB47	WB49
Major (wt.%)											
SiO_2	47.57	48.01	48.25	47.66	47.66	47.55	46.90	47.20	46.96	47.06	48.27
TiO_2	1.25	1.26	1.25	1.58	1.49	1.56	1.53	1.54	1.44	1.40	1.24
Al_2O_3	17.32	17.27	17.22	17.29	17.13	17.16	17.31	17.31	17.27	17.68	17.18
FeO	9.59	9.46	9.60	10.19	10.17	10.05	9.93	9.65	10.16	9.58	9.68
Fe_2O_3	1.72	1.70	1.73	1.83	1.83	1.81	1.79	1.74	1.83	1.72	1.74
MnO	0.13	0.14	0.14	0.15	0.14	0.14	0.14	0.14	0.14	0.14	0.14
MgO	8.54	8.30	8.21	7.99	7.79	7.70	8.24	8.31	8.48	8.43	8.40
CaO	9.53	9.34	9.30	9.21	9.38	10.06	10.09	10.17	9.39	10.05	8.67
Na_2O	3.43	3.60	3.48	3.03	3.50	3.23	3.36	3.24	3.70	3.35	3.60
K_2O	0.60	0.61	0.51	0.79	0.60	0.46	0.43	0.41	0.34	0.31	0.78
P_2O_5	0.32	0.31	0.31	0.29	0.30	0.29	0.29	0.29	0.28	0.28	0.29
Total	100.00	100.00	100.00	100.00	100.00	100.00	100.00	100.00	100.00	100.00	100.00
LOI	2.07	1.76	2.56	4.22	2.35	1.64	1.28	1.49	2.39	0.55	1.73
mg#	0.41	0.40	0.40	0.38	0.37	0.37	0.39	0.40	0.39	0.41	0.40
CIPW norms (wt.%)											
Or	3.55	3.61	3.02	4.67	3.55	2.72	2.54	2.43	2.01	1.83	4.61
Ab	24.06	25.56	27.43	25.61	25.49	25.07	22.46	23.50	23.97	23.50	26.79
An	30.05	29.12	29.82	31.20	29.22	30.92	30.84	31.44	29.47	32.25	28.38
Ne	2.67	2.64	1.07	0.00	2.21	1.20	3.21	2.10	3.95	2.61	1.97
Di	12.55	12.59	11.87	10.70	12.81	14.18	14.33	14.15	12.66	13.05	10.59
Ol	21.56	20.95	21.23	21.54	20.58	19.68	20.48	20.30	21.93	21.00	22.15
Mt	2.49	2.47	2.51	2.65	2.65	2.62	2.60	2.52	2.65	2.49	2.52
Il	2.38	2.39	2.38	3.00	2.83	2.96	2.91	2.93	2.74	2.66	2.36
Ap	0.70	0.68	0.68	0.63	0.65	0.63	0.63	0.63	0.61	0.61	0.63
Total	100.00	100.00	100.00	100.00	100.00	100.00	100.00	100.00	100.00	100.00	100.00
Trace (ppm)											
Ba	305	280	260	261	215	267	283	267	203	246	280
Rb	10	9	7	10	7	8	7	7	6	6	10
Sr	509	505	507	604	503	516	572	582	576	583	618
Y	35	37	37	31	23	33	35	34	25	37	37
Zr	150	149	149	146	142	140	147	146	145	143	155
Nb	7	7	8	8	8	8	7	8	6	5	8
V	224	222	220	242	187	253	254	259	190	247	220
Ni	168	167	175	122	94	115	140	139	114	143	165
Cr	369	364	363	315	241	324	338	334	264	334	362
Sc	39	37	32	25	26	33	32	38	25	39	34

LOI = loss on ignition; mg# = molecular MgO/(MgO+FeO); FeO and Fe_2O_3 calculated using Fe_2O_3/FeO = 0.2 from Middlemost (1989)

a primary magma derived from partial melting of a normal mantle (Irving and Green, 1976; Frey *et al.*, 1978; Wilson, 1989). The evolved nature of basalts is indicated by the relatively low concentrations of Ni (79–176 ppm) and Cr (207–369 ppm) and their Zr/TiO_2 values varying from 0.009 to 0.013 (Frey *et al.*, 1978; Wilson, 1989).

The MgO variation diagrams for major and trace elements (Figures 8 and 9) show negative trends for FeO* and TiO_2, but a positive trend for Al_2O_3. The increases in FeO* and TiO_2 with advanced fractionation are typical of either tholeiitic basalt or alkalic where the compositional trends are not significantly controlled by removal of Fe-Ti oxides (Peng and Mahoney, 1995; Temizel, 2008; Sheth *et al.*, 2012). The Al_2O_3 depletion with decreasing MgO is a clear indication that plagioclase is a major crystallizing phase along with the mafic minerals. The depletion in Ni with respect to MgO signifies that olivine is an important mafic mineral. The phenocryst and microphenocryst assemblages support the geochemically based conclusion that the minerals involved in fractionation are plagioclase and olivine. It is concluded here that the coherent basalts are evolved transitional tholeiite to alkalic have experienced a small degree of plagioclase and olivine fractionation.

The normalized REE patterns for the eight representative transitional tholeiitic basalts are shown in Figure 10. These basaltic rocks have narrow ranges of REE abundances

Table 1. Continued

Incoherent facies clasts in basalt breccias (cores)											
Sample	WB15	W16	WB18	WB20	WB24	WB26	WB28	WB31	WB33	WB37	WB39
Major (wt.%)											
SiO_2	47.37	47.88	48.84	48.65	48.69	48.98	48.04	48.91	48.80	48.59	48.75
TiO_2	1.39	1.41	1.26	1.24	1.28	1.29	1.25	1.26	1.23	1.25	1.56
Al_2O_3	17.30	17.17	17.08	17.28	17.85	17.31	17.18	16.72	16.95	17.07	17.68
FeO	9.82	9.77	9.59	9.46	9.28	9.81	9.81	9.65	9.44	9.39	10.03
Fe_2O_3	1.77	1.76	1.72	1.70	1.67	1.76	1.76	1.74	1.70	1.69	1.80
MnO	0.14	0.14	0.15	0.14	0.14	0.15	0.14	0.16	0.13	0.14	0.14
MgO	8.65	8.53	8.68	8.61	8.55	10.27	8.38	8.56	8.40	8.42	9.92
CaO	10.04	9.80	8.99	8.96	9.09	7.43	9.34	9.29	9.37	9.68	7.60
Na_2O	2.62	2.71	2.73	2.84	2.38	1.95	3.34	2.63	2.90	2.85	1.35
K_2O	0.63	0.53	0.70	0.81	0.75	0.73	0.47	0.76	0.76	0.61	0.86
P_2O_5	0.29	0.29	0.28	0.31	0.31	0.32	0.31	0.31	0.30	0.32	0.29
Total	100.00	100.00	100.00	100.00	100.00	100.00	100.00	100.00	100.00	100.00	100.00
LOI	9.80	8.13	8.56	8.33	9.70	12.76	7.26	8.71	11.29	9.43	19.24
mg#	0.41	0.40	0.41	0.41	0.42	0.45	0.40	0.41	0.41	0.41	0.43
CIPW norms (wt.%)											
Or	3.73	3.14	4.14	4.79	4.44	4.32	2.78	4.50	4.50	3.61	5.09
Ab	22.14	22.91	23.07	24.00	20.12	16.48	27.16	22.23	24.51	24.08	11.41
An	33.53	33.08	32.23	31.97	35.76	35.01	30.45	31.53	30.95	31.94	36.03
Ne	0.00	0.00	0.00	0.00	0.00	0.00	0.58	0.00	0.00	0.00	0.00
Di	14.70	17.52	20.34	16.55	23.00	32.31	11.51	22.52	17.60	18.28	40.71
Ol	20.07	17.50	14.73	17.20	11.15	6.18	21.92	13.63	16.98	16.56	0.00
Mt	2.57	2.55	2.49	2.47	2.42	2.55	2.55	2.52	2.47	2.45	2.61
Il	2.64	2.68	2.39	2.36	2.43	2.45	2.37	2.39	2.34	2.37	2.96
Ap	0.63	0.63	0.61	0.68	0.68	0.70	0.68	0.68	0.66	0.70	0.63
Total	100.00	100.00	100.00	100.00	100.00	100.00	100.00	100.00	100.00	100.00	100.00
Trace (ppm)											
Ba	269	245	252	286	295	325	261	269	287	247	342
Rb	9	9	12	13	11	14	10	12	12	10	14
Sr	616	664	504	522	532	601	455	643	575	608	603
Y	34	34	35	36	36	37	36	35	35	34	33
Zr	144	148	144	149	153	158	145	156	150	154	144
Nb	5	5	7	8	9	7	7	8	8	8	8
V	232	236	223	223	219	244	235	230	222	217	258
Ni	147	134	161	166	155	157	150	151	157	157	119
Cr	331	336	368	361	352	355	353	346	352	349	304
Sc	36	35	41	35	40	39	38	42	33	34	33

LOI = loss on ignition; mg# = molecular MgO/(MgO+FeO); FeO and Fe_2O_3 calculated using Fe_2O_3/FeO = 0.2 from Middlemost (1989)

such as the La value is in the ranges of 12.5-15.2 ppm (Table 2). The chondrite normalized REE patterns display slight REE enrichment which is typical of within-plate tholeiites, transitional tholeiites and enriched mid-ocean ridge basalts (Pearce, 1982; Shervais, 1982; Meschede, 1986; Wilson, 1989). The N-MORB normalized multi-element patterns (Pearce, 1982, and 1983) show step like patterns. Ba and Th display positive anomalies and Ta and Nb display negative anomalies (Figure 11). The significant Ta–Nb anomalies rule out an oceanic within-plate environment. This suggests that the transitional tholeiitic basalts have been erupted in a continental within-plate environment and formed at pressures less than 8 kbars (Thompson, 1972; Hughes, 1982).

The transitional tholeiitic basalts have often been compared with modern lavas from different tectonic settings in terms of their REE and N-MORB normalized patterns. In both, Figure 10 and 11, the transitional tholeiitic basalts are closely analogous to the early-middle Miocene, central Sinkhote-Alin and Sakhalin basalts from northeastern margin of the Eurasian continent which was erupted in a continental rift environment (Okamura *et al.*, 2005).

6. Origin of the Basalt Breccia

Volcanism in the study area is located in the easternmost volcanic belt in Thailand, the Loei–Phetchabun. The

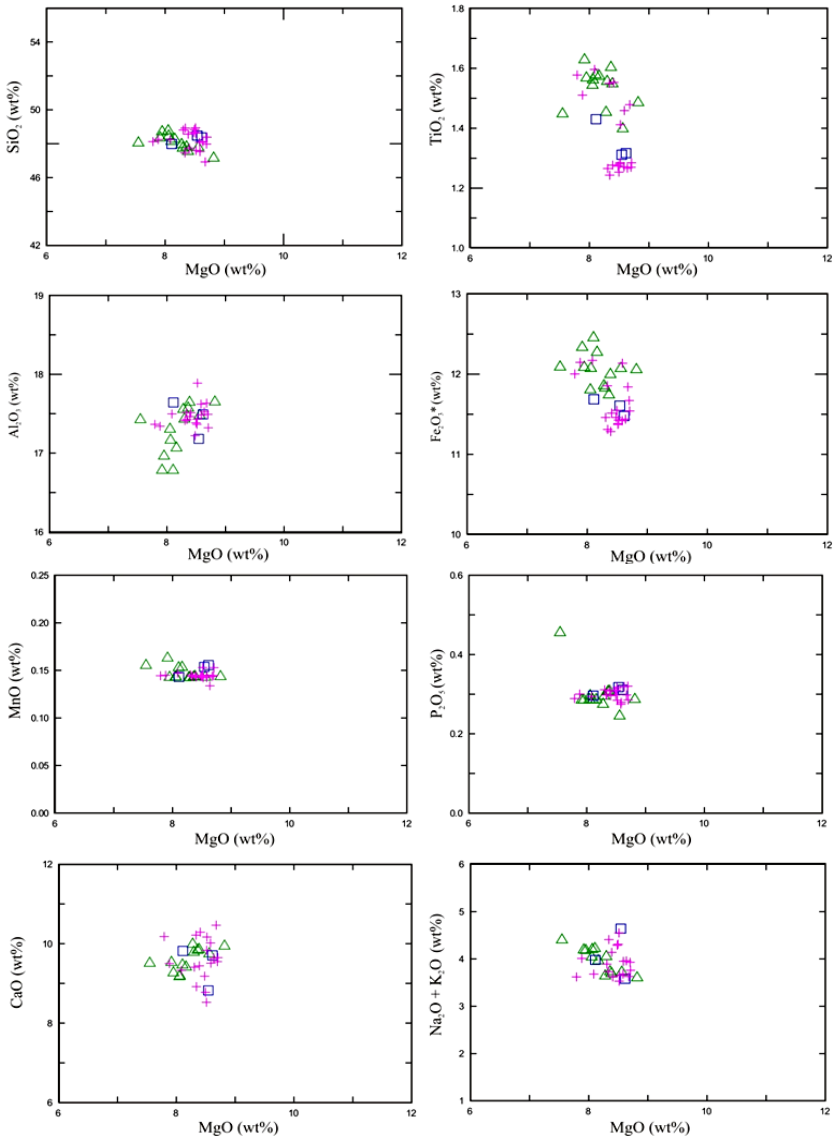

Figure 8. MgO variation diagrams of major elements for the studied basalts and the symbols used as in Figure 5.

generation of this volcanism has been correlated with the development of the Wichian Buri basin in the Late Oligocene as the result of simple shear tectonics associated with right lateral movement on the NW–SE trending the Mae Ping fault and the Three Pagoda fault, and left lateral movement along NNE–SSW trending conjugate strike slip faults (Polachan and Sattayarak, 1989; Morley, 2002).

The Wichian Buri basalts have been erupted in the Miocene (Chualaowanich *et al.*, 2008) with two main volcanic facies, coherent facies basalt and incoherent facies basalt. The similarity of coherent facies basalt and incoherent facies basalt in terms of their petrography and geochemical compositions signifies that these two facies rocks have been formed from the same continental within-plate transitional tholeiitic magma. The holocrystalline to hypohyaline groundmass of both facies rocks suggest that the coherent facies basalts had slower cooling rates than the incoherent facies basalts, which is the product of autobrecciation formed by the interaction between hot magma and cold water. The appearances of pillow lobes and pillow fragments in the study area are evidenced for subaqueous eruptions (Figure 3).

It is well recognized that two episodes of continental within plate basaltic volcanism occurred during the Tertiary worldwide (Monghazi, 2003; Abdel-Rahman and Nassar, 2004; Okamura *et al.*, 2005). The older episode commonly yielded tholeiitic basalts and transitional tholeiitic to alkalic basalts while the younger episode produced transitional tholeiitic to strongly alkalic basalts (Monghazi, 2003; Abdel-Rahman and Nassar, 2004; Okamura *et al.*, 2005). The Wichian Buri transitional tholeiitic basalts have been generated in the older episodic volcanism while to the east of the study area,

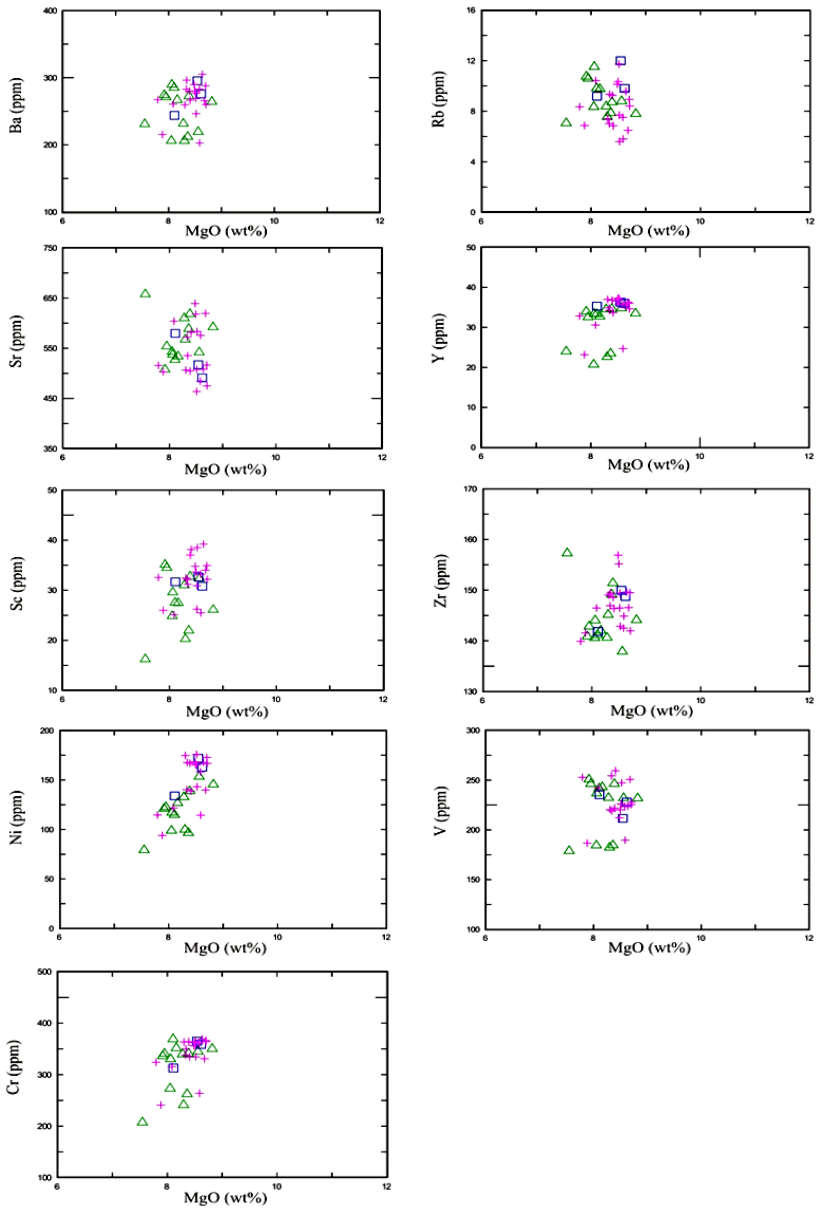

Figure 9. MgO variation diagrams of trace elements for the studied basalts and the symbols used as in Figure 5.

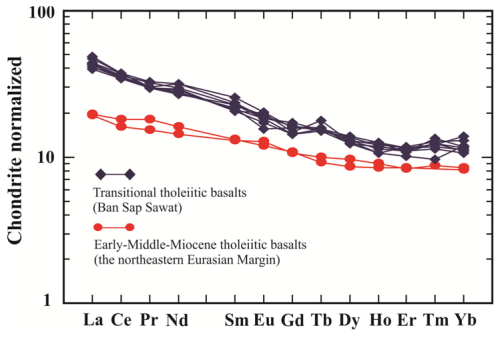

Figure 10. Plots of chondrite normalized REE patterns for the representative studied basalts and their modern analogs (Okamura *et al.*, 2005); normalizing values used are those of Taylor and Gorton (1977).

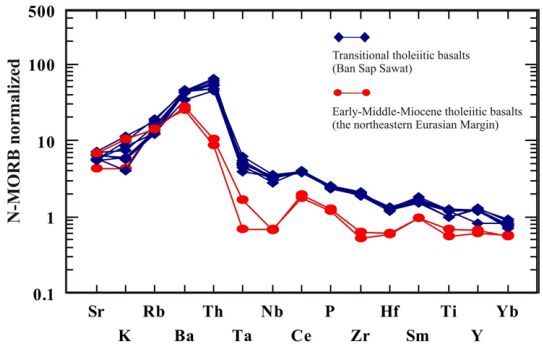

Figure 11. Plots of N-MORB normalized multi-element patterns (Pearce, 1982; 1983) for the representative studied basalts and their modern analogs (Okamura *et al.*, 2005), N-MORB normalizing values used are those of Sun and McDonough (1989).

Table 2. Rare earth elements analyses and the selected chondrite-normalized ratios of the studied basaltic rocks.

Sample	WB2	WB7	WB17	WB29	WB41	WB42	WB43	WB44
Rare earth elements (ppm)								
La	12.50	13.50	13.80	15.20	13.00	13.00	14.70	13.40
Ce	28.00	29.00	30.30	30.10	28.20	28.90	30.50	28.90
Pr	3.40	3.70	3.50	3.40	3.40	3.50	3.80	3.50
Nd	16.00	17.70	16.30	16.90	17.30	18.90	18.70	16.50
Sm	4.37	4.35	4.16	3.94	3.96	4.85	4.47	4.07
Eu	1.32	1.38	1.12	1.24	1.44	1.45	1.34	1.31
Gd	3.71	4.14	4.06	3.67	3.84	4.07	4.19	4.43
Tb	0.76	0.77	0.77	0.74	0.87	0.76	0.74	0.75
Dy	4.20	4.02	4.14	3.99	4.14	4.49	4.39	4.22
Ho	0.83	0.86	0.91	0.77	0.78	0.91	0.87	0.89
Er	2.32	2.39	2.45	2.48	2.15	2.29	2.28	2.46
Tm	0.34	0.34	0.36	0.38	0.29	0.37	0.40	0.35
Yb	2.19	2.19	2.88	2.68	2.48	2.28	2.45	2.32
Hf	2.45	2.56	2.71	2.49	2.61	2.67	2.76	2.77
Th	7.00	6.00	8.00	6.00	5.00	7.00	6.00	7.00
Ta	0.64	0.51	0.62	0.58	0.72	0.81	0.68	0.66
La/Yb_{cn}	5.70	6.16	4.79	5.67	5.24	5.70	6.00	5.77
La/Sm_{cn}	2.86	3.10	3.32	3.86	3.28	2.68	3.29	3.29
Sm/Yb_{cn}	2.00	1.99	1.44	1.47	1.60	2.13	1.82	1.75

cn = chondrite-normalized values from Taylor and Gorton (1977)

the younger episodic volcanism of alkalic basaltic magma have been erupted after in a relatively short period of time (Intasopa *et al.*, 1995; Chualaowanich *et al.*, 2008).

The origin of the Wichian Buri basalts proposed here involves two stages. A first stage generated the basaltic lava flows followed by a second stage that yielded the basalt breccias which should have occurred after the emplacement of the lava flows. The latter stage would also have produced from non explosive fragmentation of flowing lavas leading to autobreccia, equivalent to hyaloclastite. During the emplacement of the lava flows, the cores of the lava flows may be overlain by carapace of the basalt breccias.

Acknowledgements

This research was financially supported by the Thailand Research Fund (TRF) and the Office of the Higher Education Commission (OHEC). The authors thank the Department of Mineral Resources, Bangkok, Thailand for permission to the core samples. Field work was carried out with the Igneous Rocks and Related Ore Deposits Research Unit (IROU), Department of Geological Sciences, Faculty of Science, Chiang Mai University. Dr. Nick Walsh of the Department of Earth Sciences, Royal Holloway University of London is thanked for his REE analyses. Two anonymous reviewers are thanked for their helps to improve the manuscript.

References

Abdel-Rahman, A.M. and Nassar, P.E. 2004. Cenozoic volcanism in the Middle East, petrogenesis of alkali basalts from northern Lebanon. Geological Magazine. 141, 545-563.

Barr, S.M. and MacDonald, A.S. 1981. Geochemistry and geochronology of late Cenozoic basalts of Southeast Asia-part II. Geological Society of American Bulletin. 92, 1069-1142.

Ben-Avraham, Z. and Uyeda, S. 1973. Evolution of the China Basin and the Mesozoic palaeogeography of Borneo. Earth and Planetary Science Letters. 18, 365-76.

Chualaowanich, T. Saisuthichai, D. Sarapanchotewittaya, P. Charusiri, P. Sutthirat, C. Lo, C.H. Lee, T.Y. and Yeh, M.W. 2008. New $^{40}Ar/^{39}Ar$ Ages of some Cenozoic basalts from the east and northeast of Thailand. Proceedings of International Symposia on Geoscience Resources and Environments of Asian Terranes, Bangkok, Thailand, November 24-26, 2008, 225-229.

Dunning, G.R. MacDonald, A.S. and Barr, S.M. 1995. Zircon and monazite U-Pb dating of the Doi Inthanon core complex, northern Thailand: implications for extension within the Indosinian orogen. Tectonophysics. 251, 197-213.

Flower, M.F.J. Zhang, M. Chen, C.Y. Tu, K. and Xie, G. 1992. Magmatism in the South China Basin: 2. Post-spread-

ing Quaternary basalts from Hainan Island, south China. Chemical Geology. 97, 65-87.

Floyd, P.A. and Winchester, J.A. 1975. Magma type and tectonic setting discrimination using immobile elements. Earth and Planetary Science Letters. 27, 211-218.

Frey, F.A. Green, D.H. and Roy, S.D. 1978. Integrated models of basalt petrogenesis, A study of quartz tholeiites to olivine melilitites from SE Australia utilizing geochemical and experimental petrological data. Journal of Petrology. 19, 463-513.

Graham, I. Sutherland, F.L. Zaw, K. Nechaev, V. and Khanchuk, A. 2008. Advances in our understanding of the gem corundum deposits of the west pacific continental margin intraplate basaltic fields. Ore Geology Reviews. 34, 200-215.

Ho, K.S. Chen, J.C. and Juang, W.S. 2000. Geochronology and geochemistry of late Cenozoic basalts from the Leiqiong area, southern China. Journal of Asian Earth Sciences. 18, 307-324.

Hoang, N. and Flower, M.F.J. 1998. Petrogenesis of Cenozoic basalts from Vietnam: Implication for origins of a 'diffuse igneous province'. Journal of Petrology. 39, 369-395.

Hoang, N. Flower, M.F.J. and Carlson, R.W. 1996. Major, trace, and isotopic compositions of Vietnamese basalts: Interaction of hydrous EM1-rich asthenosphere with thinned Eurasian lithosphere. Geochimica et Cosmochimica Acta. 60, 4329-4351.

Hughes, C.J. 1982. Igneous petrology. Elsevier, New York, USA, pp 551.

Intasopa, S. Dunn, T. and Lambert, R.J. 1995. Geochemistry of Cenozoic basaltic and silicic magmas in the central portion of the Loei-Phetchabun volcanic belt, Lop Buri, Thailand. Canadian Journal of Earth Sciences. 32, 393-409.

Irvine, T.N. and Baragar, W.R.A. 1971. A guide to chemical classification of the common volcanic rocks. Canadian Journal of Earth Sciences. 8, 523-548.

Irving, A.J. and Green, D.H. 1976. Geochemistry and petrogenesis of the newer basalts of Victoria and South Australia. Journal of Geolological Society of Australia. 23, 45-46.

Jungyusuk, N. and Sinsakul, S. 1989. Geologic map of Nong Phai and Wichianburi districts. Geological Survey Division, Department of Mineral Resources. Bangkok, Thailand.

Kuno, H. 1966. Lateral variation of basalt magma types across continental margins and island arcs. Bulletin of Volcanology. 29, 195-222.

Lawver, L.A. Curry, J.R. and Moore, D.G. 1976. Tectonic evolution of the Andaman sea. American Geophysical Union Transactions. 75, 333.

Le Bas, M.J. Le Maitre, R.W. Streckeisen, A.L. and Zanethin, B. 1986. A chemical classification of volcanic rocks based on the total alkali-silica diagram. Journal of Petrology. 27, 745-750.

Limtrakun, P. Panjasawatwong, Y. Buasamlee, N. Boonsoong, A. Srithai, S. and Srichan, W. 2005, Petrology and geochemistry of late Cenozoic basalt from Long district, Phrae province, northern Thailand. Proceedings of International Conference on Geology, Geotechnology and Mineral Resources of Indochina, Khon Kaen, Thailand, November 28-30, 2005, 352-357.

MacDonald, G.A. 1968. Composition and origin of Hawaiian lavas. In Studies in volcanology. R.R. Coats, R.L. Hay, C.A. Anderson, editors. Geological Society of America Memoir. 11, 477-522.

McPhie, J. Doyle, M. and Allen, R. 1993. Volcanic Textures: a guide to the interpretation of textures in volcanic rocks. Tasmanian Government Printing Office, Tasmania, Australia, pp. 1-19.

Meschede, M. 1986. A method of discriminating between different types of mid-ocean ridge basalts and continental tholeiites with the Nb-Zr-Y diagram. Chemical Geology. 56, 207-218.

Middlemost, E.A.K. 1989. Iron oxidation ratios, norms and the classification of volcanic rocks. Chemical Geology. 77, 19–26.

Miyashiro, A. 1975. Classification, characteristics and origin of ophiolites. Journal of Geology. 83, 249-281.

Morley, C.K. Woganan, N. Sankumarn, N. Hoon, T.B. Alief, A. and Simmons, M. 2001. Late Oligocene-Recent stress evolution in rift basins of northern and central Thailand: implications for escape tectonics. Tectonophysics. 334, 115-150.

Morley, C.K. 2002. A tectonic model of the Tertiary evolution of strike-slip faults and rift basins in SE Asia. Tectonophysics. 347, 189-215.

Moghazi, A.M. 2003.Geochemistry of a Tertiary continental basalt suite, Red Sea coastal plain, Egypt, petrogenesis and characteristics of the mantle source region. Geological Magazine. 140, 11-24.

Okamura, S. Arculus, R.J. and Martonov, Y.A. 2005. Cenozoic magmatism of the north–eastern Eurasian margin, the role of lithosphere versus asthenosphere. Journal of Petrology. 46, 221-253.

Pearce, J.A. 1982. Trace element characteristics of lavas from destructive plate boundaries. In Andesites-Orogenic and Related Rocks, R.S. Thorpe, editor. A Page Bros, Norwich, UK.

Pearce, J.A. 1983. Role of subcontinental lithosphere in magma genesis at destructive plate margins. In Continental Basalts and Mantle Xenoliths, C.J. Hawkesworth and M.J. Norry, editors. Shiva Publishing, Norwich, UK.

Pearce, J.A. and Cann, J.R. 1973. Tectonic setting of basic volcanic rocks determined using trace element analyses. Earth and Planetary Science Letters. 19, 290-300.

Peng, Z.X. and Mahoney, J.J. 1995. Drillhole lavas from the northwestern Deccan Traps, and the evolution of Réunion hotspot mantle. Earth and Planetary Science Letters. 134, 169-185.

Polachan, S. and Sattayarak, N. 1989. Strike-slip tectonics and the development of Tertiary basins in Thailand: Aspects of sedimentary basin evolution assessed through tectonic subsidence analysis example, northern Gulf of Thailand. Journal of Southeast Asian Earth Sciences. 8, 404-420.

Shervais, J.W. 1982. Ti-V plots and the petrogenesis of modern and ophiolitic lavas. Earth and Planetary Science Letters. 59,101-118.

Sheth, H.C. Choudhary, A.K. Cucciniello, C. Bhattacharyya, S. Laisharm, R. and Gurav, T. 2012. Geology, petrochemistry, and genesis of the bimodal lavas of Osham Hill, Saurashtra, northwestern Deccan Traps. Journal of Asian Earth Sciences. 43, 176-192.

Sun, S.S. and McDonough, W.F. 1989. Chemical and isotopic systematic of oceanic basalts, implications for mantle compositions and processes. In Magmatism in ocean basins, A.D. Saunders and M.J. Norry, editors. Geological Society of London, Special Publication. 42, 313-345.

Sutherland, F.L. Bosshart, G. Fanning, C.M. Hoskin, P.W.O. and Coenraads, R.R. 2002. Sapphire crystallization, ages and origin, Ban Huai Sai, Laos: age based on zircon inclusions. Journal of Asian Earth Sciences. 20, 841-849.

Sutthirat, C. Charusiri, P. Farrar, E. and Clark, A.H. 1994. New $^{40}Ar/^{39}Ar$ geochronology and characteristics of some Cenozoic basalts in Thailand. Proceedings of international symposium on stratigraphic correlation of Southeast Asia, Bangkok, Thailand, 306-320.

Tapponnier, P., Peltzer, G. and Armiro, R. 1986. On the mechanics of the collision between India and Asia. In Collision Tectonics, M.P. Coward and A.C. Ries, editors. Geological Society of London, Special Publication. 19, 115-157.

Taylor, S.R. and Gorton, M.K. 1977. Geochemical application of spark-source mass spectrometry III, element sentivity, precision and accuracy. Geochimica et Cosmochimica Acta. 41, 1375-1380.

Temizel, I. and Arslan, M. 2008. Petrology and geochemistry of Tertiary volcanic rocks from the Ikizce (Ordu) area, NE Turkey: Implications for the evolution of the eastern Pontide paleo-magmatic arc. Journal of Asian Earth Sciences. 31, 439-463.

Thompson, R.N. 1972. Melting behavior of Snake River lavas at pressures up to 35 kb. Geophysical Laboratory Yearbook, Carnegie Institute of Washington. 71, 406-410.

Tingay, M. Morley, C.K. King, R. Hillis, R. Coblentz, D. and Hall, R. 2010. Present-day of stress field of Southeast Asia. Tectonophysics. 482, 92-104.

Tu, K. Flower, M.F.J. Carlson, R.W. Zhang, M. and Xie, G. 1991. Sr, Nd and Pb isotopic compositions of Hainan basalts (South China); implications for a subcontinental lithosphere Dupal source. Geology. 19, 567-569.

Tu, K. Flower, M.F.J. Carlson, R.W. Xie, G. Chen, C.Y. and Zhang, M. 1992. Magmatism in the south China basin: 1. Isotopic and trace-element evidence for an endogenous Dupal mantle component. Chemical Geology. 97, 47-63.

Wang, X.C. Li, X.H. Li, Z.X. Liu, Y. and Yang, Y.H. 2010. The Willouran basic province of South Australia: Its relation to the Guibei large igneous province in South China and the break up of Rhodinia. Lithos. 119, 569-584.

Wang, X.C. Li, Z.X. Li, X.H. Li, J. Liu, Y. Long, W.G. Zhou, J.B. and Wang, F. 2012. Temperature pressure, and composition of the mantle source region of late Cenozoic basalts in Hainan Island, SE Asia: A consequence of a young thermal mantle plume close to subduction zones? Journal of Petrology. 53, 177-233.

Wilson, M. 1989. Igneous petrogenesis: A global tectonic approach. Unwin Hyman, London, UK, pp 466.

Winchester, J.A. and Floyd, P.A. 1977. Geochemical discrimination of different magma series and their differentiation products using immobile elements. Chemical Geology. 20, 325-343.

Xia, L. Xiangmin, L. Zhongping, M. Xu, X. and Xia, Z. 2011. Cenozoic volcanism and tectonic evolution of the Tibetan plateau. Gondwana Research. 19, 850-866.

Yin, A. 2010. Cenozoic tectonic evolution of Asia: A preliminary synthesis. Tectonophysics. 488, 293-325.